Conductance of a quantum wire at low electron density

K. A. Matveev
Materials Science Division, Argonne National Laboratory, Argonne, Illinois 60439, USA and
Department of Physics, Duke University, Durham, North Carolina 27708, USA
(Received 23 May 2004; revised manuscript received 13 October 2004; published 23 December 2004)

We study the transport of electrons through a long quantum wire connecting two bulk leads. As the electron density in the wire is lowered, the Coulomb interactions lead to short-range crystalline ordering of electrons. In this Wigner crystal state the spins of electrons form an antiferromagnetic Heisenberg spin chain with exponentially small exchange coupling J. Inhomogeneity of the electron density due to the coupling of the wire to the leads results in violation of spin-charge separation in the device. As a result the spins affect the conductance of the wire. At zero temperature the low-energy spin excitations propagate freely through the wire, and its conductance remains $2e^2/h$. Since the energy of the elementary excitations in the spin chain (spinons) cannot exceed $\pi J/2$, the conductance of the wire acquires an exponentially small negative correction $\delta G \propto -\exp(-\pi J/2T)$ at low temperatures $T \ll J$. At higher temperatures, $T \gg J$, most of the spin excitations in the leads are reflected by the wire, and the conductance levels off at a new universal value e^2/h.

DOI: 10.1103/PhysRevB.70.245319 PACS number(s): 73.63.Nm, 73.21.Hb, 75.10.Pq

I. INTRODUCTION

The quantization of conductance of one-dimensional (1D) electron systems in units of $2e^2/h$ was first observed in experiments with quantum point contacts.[1,2] The latter consist of a short (well under 1 μm) 1D constriction connecting two bulk two-dimensional leads. Further progress in fabrication of low-disorder devices resulted in observation[3,4] of similar conductance quantization in quantum wires of several microns in length. Experimentally the quantization is observed as very flat plateaus in the dependence of linear conductance on the voltage at the gate controlling the electron density in the wire.

In a number of recent experiments[5–13] deviations of conductance from perfect quantization have been observed at low electron density. These deviations manifest themselves as negative corrections to the conductance at the beginning of the first quantized plateau. The correction is usually small at the lowest temperatures available, but becomes significant at $T \sim 1$ K. In typical samples[5–7] the conductance levels off at high temperatures and forms a quasiplateau at about $0.7 \times (2e^2/h)$. This phenomenon is often referred to as the *0.7 structure*. Despite the numerous theoretical attempts[14–26] at the interpretation of the 0.7 structure, its origin remains unclear.

The analysis of the existing experimental data shows that the 0.7 structure is sensitive to the length of the one-dimensional region connecting the two-dimensional leads. The structure tends to be relatively weak in the short contacts,[8,9] where no quasiplateau is observed even at high temperatures. On the other hand, in longer samples[10–13] the plateau is observed even at the lowest temperatures available. The effect is also somewhat stronger, with the quasiplateau moving to a lower value of conductance $G \approx 0.5 \times (2e^2/h)$.

In this paper we consider conductance of a long quantum wire in the regime of low electron density n. Focusing on the case of a GaAs device, we assume quadratic energy spectrum for free electrons $\epsilon(p) = p^2/2m$, where m is the effective mass of the electrons. The typical kinetic energy of an electron at zero temperature is of the order of the Fermi energy, $E_F = (\pi\hbar n)^2/8m$. It is important to note that at low density $n \ll a_B^{-1}$ the kinetic energy is small compared to the typical energy $e^2 n/\varepsilon$ of Coulomb interaction between electrons, where ε is the dielectric constant, and $a_B = \varepsilon\hbar^2/me^2$ is the effective Bohr radius of the material. Thus in the limit of low density the electrons can be viewed as classical particles placed at equidistant positions to minimize the Coulomb repulsion, see Fig. 1. Such a picture was first proposed by Wigner[27] and will be referred to as the *Wigner crystal*.

Although the quantum fluctuations of electrons near their equilibrium positions destroy the long-range order in the Wigner crystal, its short-range structure strongly affects the transport through the wire. In particular, the electrons occupying well-defined sites of a Wigner lattice can be viewed as an antiferromagnetic spin chain with exponentially small exchange constant J. The appearance of a new energy scale $J \ll E_F$ significantly affects the physics of the electronic transport through the wire. This effect is most important at intermediate temperatures, $J \ll T \ll E_F$, where it results in a considerable suppression of the conductance of the wire.

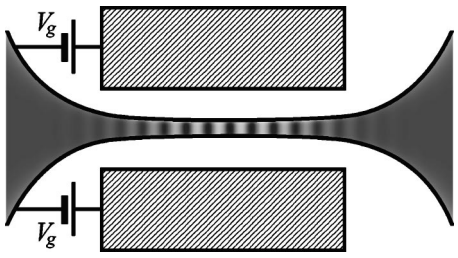

FIG. 1. Sketch of electron density in a quantum wire formed by confining two-dimensional electrons with gates (shaded). The density n of one-dimensional electrons in the wire is controlled by the gate voltage V_g. At low density $n \ll a_B^{-1}$ the electrons in the wire form a Wigner crystal.

The physics of this phenomenon is controlled by the effect of spin-charge separation in one-dimensional interacting electron systems. The latter refers to the fact that fermionic quasiparticles cannot be viewed as elementary excitations of the system, i.e., it no longer behaves as a Fermi liquid. Instead, the system displays Luttinger liquid behavior, and the elementary excitations are bosonic waves of charge and spin densities propagating at different velocities. As a result, when an electron enters the one-dimensional region from one of the leads, it is decomposed into charge and spin waves. At low temperature $T \ll J$ both waves pass through the wire, and upon reaching the other lead they reassemble into a fermionic quasiparticle. This process can be interpreted as perfect transmission of electrons through the wire and gives the standard value of conductance $G=2e^2/h$. On the other hand, at $T \gg J$, the bandwidth $D_\sigma \sim J$ of the spin excitations in the wire is small compared to their typical energy T. As a result, only the charge excitations pass through the wire, whereas the spin ones are reflected back to the lead. We show below that this additional scattering of spin excitations by the wire reduces its conductance to e^2/h.

In Sec. II we study the applicability of the Luttinger liquid description to the 1D Wigner crystal and show that it is only valid at energy scales below J. On the other hand, the property of spin-charge separation is more general and persists at energy scales above J. We review the known results for the conductance of a quantum wire in Sec. III. The most important consequence of the spin-charge separation in quantum wires is the conclusion that spin degrees of freedom do not affect the conductance, which remains quantized at $2e^2/h$. In Sec. IV we show that the spin-charge separation is violated when the wire is connected to the leads. As a result the spin subsystem affects the propagation of electric charge through the wire and contributes to its resistance. This contribution is studied in Sec. V, where we find that at $J \ll T$ the conductance of the device reduces from $2e^2/h$ to e^2/h. The relation of our results to experimental measurements of conductance of quantum wires is discussed in Sec. VI. A brief summary of some of our results has been reported in Ref. 28.

II. SPIN-CHARGE SEPARATION IN QUANTUM WIRES

It has been known since the 1970s (Ref. 29) that the low-energy excitations of a 1D system of interacting electrons are the charge and spin waves propagating independently of each other at different velocities. This result is valid at the energy scales low compared to the bandwidths D_ρ and D_σ of the charge and spin excitations. In the case of not very strong interactions both bandwidths are of the order of the Fermi energy, and the picture of completely separated charge and spin excitations is appropriate at $T \ll E_F$.

At low electron density $n \ll a_B^{-1}$ the interactions between electrons are strong. We show below that as a result the velocity of the spin excitations is greatly reduced, and their bandwidth $D_\sigma \sim J$ becomes much smaller than E_F. A similar effect is known to occur in the strong interaction limit of some lattice models, such as the Hubbard model.[30] In this regime, the description of the spin excitations in the language of noninteracting spin waves is applicable only at very low temperatures $T \ll J$. We show in this section that a generalized picture of decoupled charge and spin excitations remains valid even at $T \gtrsim J$. In this picture the charge excitations are still given by the waves of charge density (plasmons), and the spin waves are replaced with the excitations of a Heisenberg spin chain.

A. Luttinger-liquid picture of one-dimensional electrons systems

The problems involving low-energy properties of interacting 1D electron systems are conveniently described in the framework of the bosonization technique.[31,32] The first step in this approach is to linearize the spectrum of electrons near the Fermi level, thereby replacing the quadratic dispersion law $\epsilon(k)=\hbar^2k^2/2m$ with the linear one. In this *Tomonaga-Luttinger model* the electrons are separated in two branches, the left- and right-movers, with energies $\epsilon_{L,R}(k)=\hbar v_F(\mp k - k_F)$, where v_F and k_F are the Fermi velocity and Fermi wave vector. One can then present the fermionic field operators $\psi_{L,\lambda}$ and $\psi_{R,\lambda}$ in terms of fields ϕ_λ and θ_λ satisfying bosonic commutation relations $[\phi_\lambda(x), \partial_y \theta_{\lambda'}(y)]=i\pi\delta(x-y)\delta_{\lambda\lambda'}$ using the following rule:

$$\psi_{L,\lambda}(x) = \frac{\eta_{L,\lambda}}{\sqrt{2\pi\alpha}} e^{-ik_F x} e^{i\phi_\lambda(x)-i\theta_\lambda(x)}, \tag{1a}$$

$$\psi_{R,\lambda}(x) = \frac{\eta_{R,\lambda}}{\sqrt{2\pi\alpha}} e^{ik_F x} e^{-i\phi_\lambda(x)-i\theta_\lambda(x)}. \tag{1b}$$

Here $\lambda=\uparrow,\downarrow$ is the spin index, α is the short distance cutoff, and $\eta_{L,\lambda}$ and $\eta_{R,\lambda}$ are Majorana fermion operators.[32]

In terms of the bosonic variables the Hamiltonian of an interacting 1D electron system takes the form[32,33]

$$H = H_\rho + H_\sigma, \tag{2}$$

where the two terms H_ρ and H_σ describe the excitations of the charge and spin degrees of freedom, respectively, and have the forms

$$H_\rho = \int \frac{\hbar u_\rho}{2\pi} [\pi^2 K_\rho \Pi_\rho^2 + K_\rho^{-1} (\partial_x \phi_\rho)^2] dx, \tag{3}$$

$$H_\sigma = \int \frac{\hbar u_\sigma}{2\pi} [\pi^2 K_\sigma \Pi_\sigma^2 + K_\sigma^{-1} (\partial_x \phi_\sigma)^2] dx + \frac{2g_{1\perp}}{(2\pi\alpha)^2} \int \cos[\sqrt{8}\phi_\sigma(x)] dx. \tag{4}$$

Here the new bosonic fields $\phi_{\rho,\sigma}=(\phi_\uparrow \pm \phi_\downarrow)/\sqrt{2}$ and $\Pi_{\rho,\sigma} = \partial_x(\theta_\uparrow \pm \theta_\downarrow)/\pi\sqrt{2}$ satisfy the standard commutation relations $[\phi_\alpha(x), \Pi_{\alpha'}(y)]=i\delta(x-y)\delta_{\alpha\alpha'}$ and represent the excitations of the charge and spin degrees of freedom. The Hamiltonian (2)–(4) depends on five parameters determined by the interactions between electrons: velocities u_ρ and u_σ of the charge and spin excitations, dimensionless parameters K_ρ and K_σ, and the matrix element $g_{1\perp}$ of spin-flip scattering of a left-moving electron and a right-moving one. In the absence of interactions, $u_\rho=u_\sigma=v_F$, $K_\rho=K_\sigma=1$, and $g_{1\perp}=0$. The

bosonized Hamiltonian correctly describes the charge and spin excitations of the system with energies below the respective bandwidths $D_{\rho,\sigma} \sim \hbar n u_{\rho,\sigma}$.

The most interesting case of repulsive interactions corresponds to $K_\rho < 1$. The coupling constant $g_{1\perp}$ is positive and scales to zero[32,33] at low energy scales D,

$$g_{1\perp} = \frac{g_{1\perp}}{1 + \frac{g_{1\perp}}{\pi u_\sigma} \ln \frac{D_\sigma}{D}}. \tag{5}$$

The parameter K_σ renormalizes along with $g_{1\perp}$, approaching the value $K_\sigma = 1$ required by the SU(2) symmetry as $K_\sigma = 1 + g_{1\perp}/2\pi u_\sigma$, Refs. 32 and 33.

Since the sine-Gordon term in Eq. (4) vanishes at $D/D_\sigma \to 0$, the Hamiltonian (2) becomes quadratic and describes a Luttinger liquid.[31] The latter represents a stable fixed point of the problem, so the description of the system based upon the Hamiltonian (2)–(4) is expected to be valid in a broad range of interaction strengths. It is not immediately obvious, however, that the above picture is applicable at low electron density n, i.e., when the interactions are so strong that the electrons form a Wigner crystal. Indeed, a Fourier expansion of the wave function of an electron localized in a small region of size $a \ll n^{-1}$ near a given lattice site involves the wave vectors in a broad range $\delta k \sim 1/a \gg n \sim k_F$. Thus the standard procedure of linearization of the electronic spectrum near k_F leading to the Tomonaga-Luttinger model is not justified in this case. In addition, each electron is constructed out of waves with both positive and negative wave vectors, and the picture of two separate branches of left- and right-moving particles is not applicable to the Wigner crystal. We show now that even though the conventional derivation leading to Eqs. (2)–(4) is not justified, this Hamiltonian does describe the low-energy properties of a 1D Wigner crystal.

B. Charge and spin excitations in a Wigner crystal

At low electron density, $na_B \ll 1$, the properties of the system are dominated by the Coulomb repulsion, and the electrons occupy fixed positions on the Wigner lattice. The first correction to this picture is due to the small vibrations of the lattice, analogous to phonons in conventional crystals. In the long-wavelength limit these phonons can be described in the framework of elasticity theory. In this approach the crystal is viewed as an elastic medium. Its motion is described in terms of the displacement $u(x)$ of the medium at point x from its equilibrium position and the momentum density $p(x)$. The energy of the system can then be written as a sum of kinetic and potential energies,

$$H = \int \left[\frac{p^2}{2mn} + \frac{1}{2} mns^2 (\partial_x u)^2 \right] dx. \tag{6}$$

The second term here is $1/2(\partial^2 E/\partial n^2)(\delta n)^2$, where E is the energy of the resting medium per unit length, and the density perturbation δn is proportional to the deformation of the medium, $\delta n = -n\partial_x u$. The parameter $s = \sqrt{(n/m)(\partial^2 E/\partial n^2)}$ has the meaning of the speed of density waves (plasmons) in the Wigner crystal.

The speed of plasmons in a 1D system with true Coulomb interactions between electrons diverges in the limit of long wavelength. In practice, however, the interactions between electrons are usually screened at large distances by a remote metal gate. In the model where the gate is a conducting plane at a large distance $d \gg n^{-1}$ from the Wigner crystal, the speed of plasmons is

$$s = \sqrt{\frac{2e^2 n}{\varepsilon m} \ln(\zeta n d)}, \tag{7}$$

where $\zeta \approx 8.0$, Ref. 34.

The classical Hamilton function (6) can be quantized by imposing commutation relations $[u(x), p(y)] = i\hbar\delta(x-y)$. The resulting Hamiltonian describes the propagation of the electron density excitations in a Wigner crystal, and is completely analogous to the term H_ρ in the Hamiltonian (2)–(4) of the Luttinger liquid. Comparing the commutation relations of the bosonic fields entering Hamiltonians (3) and (6), and taking into account the expressions for the density perturbation $\delta n = -(\sqrt{2}/\pi)\partial_x \phi_\rho = -n\partial_x u$, we identify the fields as

$$u(x) = \frac{\sqrt{2}}{\pi n} \phi_\rho(x), \quad p(x) = \frac{\pi n \hbar}{\sqrt{2}} \Pi_\rho(x). \tag{8}$$

Using these expressions we can relate the parameters in the Hamiltonian H_ρ to the properties of the Wigner crystal as follows

$$u_\rho = s, \quad K_\rho = \frac{v_F}{s}. \tag{9}$$

Here $v_F = \pi\hbar n/2m$ is the Fermi velocity in a noninteracting Fermi gas of density n.

The electrons in a Wigner crystal are repelled from each other by strong Coulomb forces. In the harmonic chain approximation we used so far the electrons are allowed to move about their equilibrium positions; however, the amplitude of these oscillations remains small. As a result the electrons never move from one site on the Wigner lattice to another, and can be viewed as distinguishable particles. Therefore the energy of the Wigner crystal state in this approximation does not depend on the electron spins.

To account for the spin dependence, one has to include the processes in which electrons tunnel through the Coulomb potential repelling them. Considering a pair of electrons at two neighboring sites of the Wigner lattice, one notices that depending on their total spin, the two electrons occupy either a symmetric or an antisymmetric state in the respective double-well potential. Thus the energy of the pair contains a term $J\boldsymbol{S}_1 \cdot \boldsymbol{S}_2$, where $J > 0$ is the difference of energies of the antisymmetric and symmetric states, and $\boldsymbol{S}_i$ are the operators of electron spins.[35] Taking into account all the nearest neighbor sites, we find that the spin properties of the Wigner crystal are described by the Hamiltonian of an antiferromagnetic Heisenberg spin chain

$$H_\sigma = \sum_l J \boldsymbol{S}_l \cdot \boldsymbol{S}_{l+1}. \tag{10}$$

Since the exchange is due to tunneling, the constant J is exponentially small,

$$J = J^* \exp\left(-\frac{\eta}{\sqrt{na_B}}\right). \tag{11}$$

To accurately evaluate J one has to take into account the fact that when two neighboring electrons tunnel through the Coulomb barrier separating them, all other electrons also move. Häusler[36] suggested an approximation that neglects the motion of other electrons; his result corresponds to the value of $\eta \approx 2.87$ in a finite chain of 15 electrons. We solve this model in the case of an infinite chain in Appendix A and obtain the value of $\eta \approx 2.82$. We also estimate the prefactor as

$$J^* \approx 1.79 \frac{E_F}{(na_B)^{3/4}}, \tag{12}$$

where $E_F = (\pi\hbar n)^2/8m$ is the Fermi energy of a noninteracting electron gas of density n.

The spin part (10) of the Hamiltonian of a 1D Wigner crystal is very different from that of a weakly interacting electron gas, Eq. (4). It is easy to show, however, that at low energies $D \ll J$ the two Hamiltonians are equivalent. To accomplish that we use the standard procedure[32,33] of bosonization of spin chains. The first step is to perform the Jordan-Wigner transformation

$$S_l^z = a_l^\dagger a_l - \frac{1}{2}, \quad S_l^x + iS_l^y = a_l^\dagger \exp\left(i\pi \sum_{j=1}^{l-1} a_j^\dagger a_j\right), \tag{13}$$

which expresses the spin operators in terms of creation and destruction operators $a^\dagger$ and a of spinless fermions. In terms of these operators the Hamiltonian (10) becomes

$$H_\sigma = \frac{1}{2}\sum_l J\left[(a_l^\dagger a_{l+1} + a_{l+1}^\dagger a_l) + 2\left(a_l^\dagger a_l + \frac{1}{2}\right)\left(a_{l+1}^\dagger a_{l+1} + \frac{1}{2}\right)\right]. \tag{14}$$

Thus the Heisenberg spin chain (10) is equivalent to the model (14) of interacting lattice fermions.

The second step is to bosonize the Hamiltonian (14). At low energies one can replace the lattice model (14) with a continuous one, $a_l \to a(y)$, linearize the spectrum of the fermions near the Fermi level, and then apply a bosonization transformation

$$a_{L,R}(y) = \frac{\eta_{L,R}}{\sqrt{2\pi\alpha}} e^{\mp ik_F y} e^{\pm i\phi_\sigma(y)/\sqrt{2} - i\sqrt{2}\theta_\sigma(y)}. \tag{15}$$

The resulting bosonized Hamiltonian of the spin chain is equivalent[37] to Eq. (4). The value of the speed u_σ of the spin excitations is easily deduced from the Bethe ansatz solution[38,39] of the Heisenberg model,

$$u_\sigma = \frac{\pi J}{2\hbar n}. \tag{16}$$

Thus we have established that the bosonized Hamiltonian (2)–(4) adequately describes the low-energy properties of not only weakly interacting electron systems, but also of a 1D Wigner crystal state at $na_B \ll 1$. However, it is important to keep in mind that the applicability of the bosonized description to the Wigner crystal is limited to very low temperatures $T \ll J$. Given the exponential dependence (11) of the exchange constant on density, this condition can be easily violated even at fairly low temperatures. In this case one has to use the more complicated form (10) of the Hamiltonian H_σ. We show in Sec. V that this breakdown of the Luttinger liquid picture gives rise to significant deviations of conductance of quantum wires from the quantized value $2e^2/h$.

C. Spin-charge separation at ultralow electron densities

The Wigner crystal picture discussed in Sec. II B relies on the long-range nature of the Coulomb interaction potential $V(x) = e^2/\varepsilon|x|$. In general, a 1D electron system forms a Wigner crystal state at $n \to 0$ only if the interaction potential decays slower than $1/|x|^2$ at $x \to \infty$. Indeed, for potential $V(x) \propto 1/|x|^\gamma$ the interaction energy of two electrons at the typical interparticle distance n^{-1} is $V \propto n^\gamma$, whereas the kinetic energy $E_F \propto n^2$. Thus at $\gamma > 2$ the interaction energy is negligible at $n \to 0$.

The electron density in quantum wires is usually controlled by applying voltage to metal gates. The presence of a gate affects the electron-electron interactions at large distances. For instance, if the gate is modeled by a conducting plane at a distance d from the wire, the interactions between electrons become

$$V(x) = \frac{e^2}{\varepsilon}\left(\frac{1}{|x|} - \frac{1}{\sqrt{x^2 + (2d)^2}}\right). \tag{17}$$

The screening of the Coulomb potential by the gate reduces the potential (17) to $V(x) = 2e^2d^2/\varepsilon|x|^3$ at large $|x|$. Therefore, the Wigner crystal picture fails in the limit $n \to 0$. Comparing the interaction potential at the interparticle distance $V(n^{-1})$ with the Fermi energy of electrons, one concludes that within the model (17) the Wigner crystal state exists only in the density range $a_B/d^2 \ll n \ll a_B^{-1}$.

As long as the system is in the Wigner crystal state, its spin excitations are described by the Heisenberg model (10). However, the expression (11) for the coupling constant J relies on the pure Coulomb interaction between electrons. In the case of interaction potential screened by the gate, the exponential decrease of J with decreasing density stops at $n \sim d^{-1}$, because the potential falls off rapidly at distances $x \gg d$. Using the method described in Appendix A, one estimates

$$J \sim E_F \left(\frac{nd^2}{a_B}\right)^{3/4} \exp\left(-\tilde{\eta}\sqrt{\frac{d}{a_B}}\right) \tag{18}$$

at $a_B/d^2 \ll n \ll d^{-1}$. In the case of interaction potential (17) the constant $\tilde{\eta} \approx 8.49$.

The distance to the gate in quantum wire devices is typically large, $d \gtrsim 10a_B$, and most experiments are performed at

densities well above a_B/d^2. However, if the density is reduced to $n \lesssim a_B/d^2$, the Wigner crystal picture used in Sec. II B will fail. It is interesting to explore to what extent the conclusions of Sec. II B will be affected. To this end, let us now study the limit $nd^2/a_B \to 0$.

At $n \ll a_B/d^2$ the interaction between two particles at a typical distance n^{-1} is small compared to their kinetic energy $\sim E_F$. On the other hand, when the distance between electrons is sufficiently short, $|x| \lesssim n^{-1}(nd^2/a_B)^{1/3} \ll n^{-1}$, they experience strong repulsion $V(x) \gtrsim E_F$. Thus in the limit of low electron density one can model the interaction potential (17) by short-range repulsion

$$V(x) = \mathcal{V}\delta(x). \tag{19}$$

Contrary to a naive expectation, the constant $\mathcal{V}$ should not be chosen as the integral of the interaction potential (17). Indeed, the exchange coupling of the spins of two neigboring electrons is caused by tunneling through the barrier (17). Thus to ensure that the potentials (17) and (19) result in the same exchange coupling between electrons, the parameter $\mathcal{V}$ should be chosen in such a way that the barriers (17) and (19) have equal transmission coefficients. This condition gives

$$\mathcal{V} \sim \frac{\hbar^2 a_B}{md^2} \exp\left(\tilde{\eta}\sqrt{\frac{d}{a_B}}\right). \tag{20}$$

The exponentially large value of $\mathcal{V}$ reflects the fact that the strong repulsion (17) leads to almost perfect backscattering of electrons off each other.

At $\mathcal{V} \to \infty$ the electrons are separated by thin hard-core potentials. In this limit they can be viewed as distinguishable particles, and the eigenvalues of energy become independent of the electron spins. The wave functions of the system essentially coincide with the Slater determinants for spinless noninteracting fermions. Upon bosonization, the Hamiltonian H_ρ of this system takes the form (3). The plasmon velocity s in this system is the Fermi velocity of noninteracting electron gas of density n, which is twice the Fermi velocity of nonpolarized electron gas, $s=2v_F$. Thus according to Eq. (9) we have[40] $K_\rho = 1/2$. Additional properties of this model were recently discussed in Refs. 41 and 42.

At large finite $\mathcal{V}$ the electrons can change places as a result of scattering, and the energy acquires a weak dependence on the spins. This dependence can be deduced from the well-known properties of the one-dimensional Hubbard model. It has been shown by Ogata and Shiba[43,44] that at $U/t \to \infty$ the spin and charge excitations of the Hubbard model are completely separated, with the Hamiltonian of spin excitations taking the form of the Heisenberg model (10). (Here U is the energy of the on-site repulsion in the Hubbard model, and t is the hopping matrix element.) The magnitude of the exchange constant in this Hamiltonian was found[44] to be

$$J = \frac{4t^2}{U} n_e \left(1 - \frac{\sin 2\pi n_e}{2\pi n_e}\right), \tag{21}$$

where n_e is the average number of electrons per site. In the limit $n_e \to 0$ the Hubbard model is equivalent to an electron gas with quadratic spectrum and pointlike interaction (19). The limiting procedure can be performed by introducing infinitesimal lattice period a in the Hubbard model, identifying the parameters $t=\hbar^2/2ma^2$, $U=\mathcal{V}/a$, $n_e=na$, and taking the limit $a \to 0$. Applying this procedure to the formula (21), we find

$$J = \frac{2\pi^2}{3} \frac{\hbar^4 n^3}{m^2 \mathcal{V}}. \tag{22}$$

Using the estimate (20) of parameter $\mathcal{V}$ for the interaction potential (17), we find

$$J \sim E_F \frac{nd^2}{a_B} \exp\left(-\tilde{\eta}\sqrt{\frac{d}{a_B}}\right). \tag{23}$$

Note that the results (18) and (23) for the exchange constant are of the same order of magnitude at $n = a_B/d^2$.

So far we have demonstrated that the description of the system in terms of the Hamiltonian in spin-charge separated form $H=H_\rho+H_\sigma$, with H_ρ and H_σ given by Eqs. (3) and (10) is valid in two different regimes. The first one is the Wigner crystal state at electron densities in the range $a_B/d^2 \ll n \ll a_B^{-1}$, and the second is the low density limit $n \ll a_B/d^2$, where the picture of pointlike interactions (19) is applicable. One can show[45] that in fact this picture of spin-charge separation holds at any density $n \ll a_B^{-1}$, including the regime $n \sim a_B/d^2$.

The exchange constant J in the effective spin chain Hamiltonian (10) monotonically decreases as the electron density n is lowered. In the most interesting range of densities $d^{-1} \ll n \ll a_B^{-1}$ the dependence of exchange on n is exponential, Eq. (11). At lower densities the dependence becomes a power-law one. Specifically, in the density ranges $a_B/d^2 \ll n \ll d^{-1}$ and $n \ll a_B/d^2$ one can use the estimates (18) and (23), respectively.

For the sake of simplicity, in the following sections we assume that the electron density is in the range $a_B/d^2 \ll n \ll a_B^{-1}$, and refer to the electron system as a Wigner crystal. However, all of our conclusions remain valid at any densities $n \ll a_B^{-1}$, if the value of the exchange constant J is adjusted as discussed in this section.

III. CONDUCTANCE OF A QUANTUM WIRE WITH SPIN-CHARGE SEPARATION

The spin-charge separation has a profound effect on the conductance of quantum wires. Indeed, the electric field applied to the wire couples to the electron charges and has no effect on spins. As a result, the spin degrees of freedom remain decoupled from charge ones, and the rather complex form of the Hamiltonian H_σ has no effect on the conductance. In this section we review the known results for the conductance of a quantum wire with spin-charge separation.

A. Infinite wire

Conductance of an infinite Luttinger liquid is given by $G=2K_\rho e^2/h$. This result was obtained[46,47] by assuming that a weak electric field is applied to a small part of the wire, and

the conductance was evaluated by using the Kubo formula. In the following sections it will be more convenient to evaluate the conductance of the Wigner crystal in the regime of applied current. It is therefore instructive to reproduce the result $G=2K_\rho e^2/h$ in this approach.

Let us consider a quantum wire whose charge dynamics is described by the Hamiltonian (3), and enforce the current $I=I_0\cos\omega t$ at $x=0$. By doing so we impose a boundary condition upon the charge field $\phi_\rho(0,t)$. Indeed, the bosonization expression for the electric current is $I=e(\sqrt{2}/\pi)\dot{\phi}_\rho$. [In the case of a Wigner crystal, this can be checked by using Eq. (8) and the definition $I=en\dot{u}$ of current in terms of the velocity $\dot{u}$ of the crystal.] Thus the field ϕ_ρ satisfies the condition

$$\phi_\rho(0,t)=\frac{\pi}{\sqrt{2}}q(t), \tag{24}$$

where the function

$$q(t)=\frac{I_0}{e\omega}\sin\omega t \tag{25}$$

is related to the current as $I=e\dot{q}$ and has the meaning of the number of electrons that passed through point $x=0$ at time t.

By imposing a time-dependent boundary condition (24) we drive the system with an external oscillating force. This leads to emission of plasmon waves and dissipation of the energy from the driving force to the infinite Luttinger liquid. We will find the resistance of the wire R_ρ by evaluating the energy W dissipated in unit time and comparing the result with the Joule heat law $W=\frac{1}{2}I_0^2R_\rho$. We present a formal derivation in Appendix B; here we limit ourselves to a simple semiclassical argument.

Solving the Hamilton equations with Hamiltonian (3) and boundary condition (24) we find[48]

$$\phi_\rho(x,t)=\frac{\pi I_0}{\sqrt{2}e\omega}\sin\omega(t-|x|/u_\rho), \tag{26a}$$

$$\Pi_\rho(x,t)=\frac{I_0}{\sqrt{2}eK_\rho u_\rho}\cos\omega(t-|x|/u_\rho). \tag{26b}$$

Substituting this solution back into Eq. (3), we find the following expression for the time-averaged energy density in the Luttinger liquid,

$$\langle E\rangle_t=\frac{\pi\hbar}{4e^2}\frac{I_0^2}{K_\rho u_\rho}. \tag{27}$$

The plasmon wave (26) carries the energy $\langle E\rangle_t$ at speed u_ρ in two directions. Thus the total energy dissipated into plasmon waves in unit time is given by $W=2u_\rho\langle E\rangle_t$. Comparing this result with $W=\frac{1}{2}I_0^2R_\rho$, we find the resistance

$$R_\rho=\frac{h}{2K_\rho e^2}, \tag{28}$$

in agreement with the result for the conductance found in Refs. 46 and 47.

B. Finite-length quantum wire between two noninteracting leads

The result $G=2K_\rho e^2/h$ indicates that in a quantum wire with repulsive interactions conductance should be below the quantized value $2e^2/h$. Furthermore, it is expected to decrease as the electron density n is lowered. However, the experiments consistently show perfect quantization[49] of conductance at $2e^2/h$ in a broad range of n.

This controversy was resolved[51–53] by noticing that instead of an infinite quantum wire, the experiments study transport through a finite-length wire connecting two bulk leads. Since the leads are not one-dimensional, their properties are not adequately described by the Luttinger liquid model (2)–(4). Instead, the electrons in the leads are expected to be in a Fermi liquid state.

To find the conductance of such devices, one can model[51–53] the leads connected to the wire by two semi-infinite noninteracting wires. In this model the system remains one-dimensional, but the interactions are nonvanishing only in the central part of the system. The length L of the interacting part is identified with the length of the wire. Assuming that the interactions fall off gradually at $x\to\pm\infty$, one can neglect the backscattering of electrons from the interacting region. In this limit the charge dynamics is still described by the Hamiltonian (3), but the parameters K_ρ and u_ρ become functions of coordinate x.

The measurements of dc conductance in experiments are conducted at very low frequencies $\omega\ll u_\rho/L$. The wavelength of the plasmons of frequency ω emitted in the system is then much greater than the length of the interacting region L. Thus the plasmons are emitted in the regions with $|x|\gg L$, and one should use in Eq. (28) the value of the parameter K_ρ taken at $x\to\pm\infty$. Electrons in those regions do not interact with each other, which corresponds to $K_\rho=1$. The resistance (28) of the device then becomes

$$R_\rho=\frac{h}{2e^2}, \tag{29}$$

and the perfect quantization is restored. Careful treatments[51–53] of the problem lead to the same conclusion.

IV. VIOLATION OF SPIN-CHARGE SEPARATION IN QUANTUM WIRE DEVICES

As we saw in Sec. III, the inhomogeneity of the system caused by coupling of the wire to the leads changes the conductance from $2K_\rho e^2/h$ to $2e^2/h$. This conclusion was derived from consideration of the charge excitations only, as the spin degrees of freedom were assumed to be completely separated. We now turn to the effect of the inhomogeneity on the spin part H_σ of the Hamiltonian.

We assume that the central part of the wire contains a purely one-dimensional electron system at low density $n\ll a_B^{-1}$, so that the Wigner crystal model is appropriate. The wire is also assumed to be smoothly connected to the leads, where the effective interactions are weak. This is due to several effects. First, the electron density grows as one moves away from the wire into the leads. This effectively reduces

the interaction strength, as the latter is characterized by parameter $(na_B)^{-1}$. In addition, the wire becomes wider when it couples to the leads. As a result, when two electrons arrive at the same coordinate x along the wire, they are no longer as close to each other as in the middle of the wire. This reduces the strength of interactions between 1D electrons. The two mechanisms have very similar effect on the Hamiltonian H_σ. For simplicity, in the following we limit our discussion to the effect of inhomogeneous electron density.

Following the ideas of Refs. 51–53, we model the wire connected to the leads by an inhomogeneous 1D system. The main source of inhomogeneity is the dependence $n(x)$ of the electron density on position. We assume that the density takes a constant value $n(x)=n$ inside the wire, i.e., at $|x|<L/2$, and gradually grows to a very large value $n_\infty \gg a_B^{-1}$ at $x \to \pm\infty$.

In experimental devices the dependence of electron density on the coordinate along the wire is caused by inhomogeneity of the external confining potential. Apart from changing the electron density, the external potential may also lead to backscattering of electrons in the wire. In a sufficiently long wire such processes may greatly suppress the conductance at low temperature.[46,47] In the Wigner crystal picture this phenomenon is interpreted as pinning of the crystal by the external potential.[34] On the other hand, the best available experiments show good quantization of conductance, indicating that the backscattering remains negligible. This is most likely the result of smoothness of the confining potential. Indeed, the backscattering involves the change of the electron wave vector by $2k_F$. Thus an external potential that is smooth at the scale of interparticle distance n^{-1} will cause exponentially weak backscattering. In this paper we assume that the external potential is sufficiently smooth, so that the backscattering can be neglected.

Under the above conditions the low-energy properties of the system may be described by the bosonized Hamiltonian (2)–(4), but with position-dependent parameters $u_{\rho,\sigma}$, $K_{\rho,\sigma}$, $g_{1\perp}$. In this paper we assume that the temperature is small compared with the bandwidth $D_\rho \sim \hbar n u_\rho$ of the Hamiltonian H_ρ, so that the discussion of the effect of the charge modes on the conductance presented in Sec. III is valid. On the other hand, we will be interested in the case of temperature comparable with the bandwidth $D_\sigma \sim J$ of the Hamiltonian H_σ. In this regime the bosonized version (4) of H_σ is not applicable, and one should instead use the Heisenberg model (10).

Since the exchange constant (11) strongly depends on the electron density $n(x)$, the parameter J in Eq. (10) should also be considered position-dependent. In particular, the strength of the exchange coupling between the two spins at the neighboring sites l and $l+1$ of the Wigner lattice is a function of the coordinate x_l of the lth electron: $J=J(x_l)$. It is important to note that in the presence of electric current I the Wigner lattice moves, so the coordinate x_l of the lth lattice site depends not only on l, but also on time.

The time dependence of x_l can be accounted for by noting that if during the time interval t a number $q(t)$ of electrons have moved from the left lead to the right one, the lth site of the lattice has shifted to the $(l+q)$-th position. Thus the time dependence of the positions of the lattice sites can be accounted for by replacing $l \to l+q(t)$, and the Hamiltonian H_σ takes the form

$$H_\sigma = \sum_l J[l+q(t)]\boldsymbol{S}_l \cdot \boldsymbol{S}_{l+1}. \tag{30}$$

Note that in this approximation the electric current $I=e\dot{q}(t)$ is assumed to be uniform throughout the wire. This is true in the dc limit $\omega \ll u_\rho/L$.

It is important to note that the form (30) of the Hamiltonian H_σ violates the spin-charge separation. Indeed, the coupling between the spins depends on the amount of charge that passed through the wire, which is related to the field ϕ_ρ, see Eq. (24). As a result, the conductance of a quantum wire connected to bulk leads may be affected by the spin excitations.[54]

To find the effect of spin subsystem on the conductance, one could substitute the expression (24) for $q(t)$ into Eq. (30), and consider the complete Hamiltonian $H_\rho + H_\sigma$ without relying on spin-charge separation. In this approach one needs to add to the Hamiltonian a term describing the applied bias, and evaluate the electric current. However, it is more convenient to treat the current $I(t)$ in the wire as an external parameter. In this case $q(t)$ is also a parameter, and the Hamiltonians H_ρ and H_σ still commute. The only consequence of the violation of spin-charge separation in this approach is the dependence of H_σ on the current $I(t)$.

The presence of an oscillating parameter (25) in the Hamiltonian (30) may lead to the creation of spin excitations. Using the approach of Sec. III, we will calculate the energy dissipated into spin excitations in unit time. In the limit of weak current, the dissipation is found in the second order of the perturbation theory in the amplitude I_0 of current oscillations. Thus in addition to the plasmon result for the energy W dissipated in unit time, we will obtain a similar contribution of the spin modes:

$$W = \frac{1}{2}I_0^2 R_\rho + \frac{1}{2}I_0^2 R_\sigma. \tag{31}$$

Comparing this result with the Joule heat law $W=\frac{1}{2}I_0^2 R$, we conclude that the resistance R of the wire is given by the sum of two independent contributions,

$$R = R_\rho + R_\sigma. \tag{32}$$

Note that the first term in this expression is already known, Eq. (29). The second term is discussed in Sec. V.

It is interesting to point out that the result (32) may be interpreted as a total resistance of the charge and spin subsystems connected in series, whereas naively one might expect a parallel connection. The reason is that the spins do not directly respond to the applied voltage, as required for the latter interpretation. Instead, the spin subsystem responds to the electric current. Thus the Hamiltonians H_ρ and H_σ become independent in the regime of applied current, in analogy with the problem of two independent resistors connected in series. A result similar to Eq. (32) has been obtained for the resistivity of two-dimensional strongly interacting systems in Ref. 55.

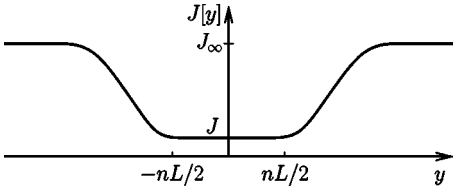

FIG. 2. Sketch of the dependence $J[y]$ in our model. Inside the wire, $|y|<nL/2$, the exchange J is exponentially small, Eq. (11). As one moves toward the leads, J grows, and at $y\to\infty$ it saturates at $J_\infty\sim E_F$.

V. SPIN CONTRIBUTION TO THE RESISTANCE

To find the contribution R_σ of the spin subsystem to the resistance of the device, we study the dissipation of energy into spin excitations caused by the time dependence of the Hamiltonian (30). We start by performing the Jordan-Wigner transformation (13) and converting the Hamiltonian to the fermionic form

$$H_\sigma=\frac{1}{2}\sum_l J[l+q(t)]\Big[(a_l^\dagger a_{l+1}+a_{l+1}^\dagger a_l)+2\Big(a_l^\dagger a_l+\frac{1}{2}\Big)\Big(a_{l+1}^\dagger a_{l+1}+\frac{1}{2}\Big)\Big]. \tag{33}$$

In the absence of the external magnetic field the average z-component of the spin at every site of the lattice must vanish. Thus according to Eq. (13) the occupation of each site is $\langle a_l^\dagger a_l\rangle=\frac{1}{2}$. This means that the Fermi level is in the middle of the band, $\mu=0$.

The exchange $J[y]$ strongly depends on the position y. Inside the wire the electron density is low, $na_B\ll 1$, and the exchange is exponentially small, Eq. (11). As the wire connects to the bulk leads, the density $n(x)$ begins to grow. At $na_B\sim 1$ the exchange J becomes of the order of the Fermi energy, see Eqs. (11) and (12).

Strictly speaking, the Wigner crystal picture is valid only at $na_B\ll 1$, i.e., as long as $J\ll E_F$. On the other hand, we will be interested in the properties of the system at low energies $D\ll E_F$. Thus at $J\sim E_F$ when the Wigner crystal picture fails, we are only concerned with the energy scales much lower than J. As we saw in Sec. II, at those scales one can use the bosonized Hamiltonian (4) regardless of the applicability of the Wigner crystal description. Thus we can ignore the difference between the Wigner crystal and weakly interacting electron gas at large density $n\gg a_B$, and simply assume that in the leads the exchange J saturates at $J_\infty\sim E_F$.

The properties of the function $J[y]$ can thus be summarized as follows:

$$J[y]=\begin{cases} J\ll E_F & \text{at } |y|<nL/2,\\ J_\infty\sim E_F & \text{at } |y|\to\pm\infty,\end{cases} \tag{34}$$

see Fig. 2. Note that y is the coordinate on the Wigner lattice. Since we consider the limit of very smooth confining potential, all the physical quantities change very little at the interparticle distance. We therefore assume that $J[y]$ is a slowly varying function: $|dJ/dy|\ll J[y]$.

A. *XY* model

The Hamiltonian (33) describes a system of strongly interacting fermions. As a first approximation we will simplify the problem by neglecting the interactions between the fermions,

$$H_\sigma^{XY}=\frac{1}{2}\sum_l J[l+q(t)](a_l^\dagger a_{l+1}+a_{l+1}^\dagger a_l). \tag{35}$$

This Hamiltonian corresponds to the fermionized version of the *XY* model of a spin chain, in which the coupling of the z-components of spin operators is neglected. This approximation violates the SU(2) symmetry of the problem, and is therefore rather crude. On the other hand, the resistance R_σ can be found exactly for model (35), and the result will provide considerable insight into the properties of model (33).

Hamiltonian (35) represents an inhomogeneous version of the tight-binding model of lattice fermions. In the uniform case, $J[y]=\text{const}$, the spectrum is well known,

$$\epsilon(k)=J\sin k, \tag{36}$$

where the wave vector k is measured from $k_F=\pi/2$. One can either assume that k varies in the interval $-\pi<k<\pi$, or choose $0<k<\pi$ and treat Eq. (36) as spectra of two branches of excitations, the particles and holes.

In the absence of electric current in the wire one can omit $q(t)$ in the Hamiltonian (35) and view it as a tight-binding model with slowly varying bandwidth $2J[y]$. In the leads the bandwidth $2J_\infty$ is very large; it narrows down to a very small value $2J$ in the wire, Eq. (34). The particles moving toward the wire in one of the leads cross to the other lead if their energies are below the small exchange J in the wire; the particles with $\epsilon>J$ are reflected.

In the presence of the electric current I, the constriction of the band in the Hamiltonian (35) moves with respect to the lattice with velocity $\dot q=I/e$. The particles reflected from the moving constriction change their energy. These processes lead to the dissipation of energy and contribute to the resistance R_σ.

For noninteracting fermions, the problem of evaluating the energy W dissipated in unit time by a moving scatterer can be solved for arbitrary reflection coefficient $\mathcal{R}(\epsilon)$, see Appendix C. Here we find W in the semiclassical limit, which is valid for very slowly varying bandwidth $J[y]$, when $\mathcal{R}(\epsilon)=\theta(\epsilon-J)$.

In the limit of slowly varying $J[y]$ one can apply the result (36) for the spectrum of particles at every point in space, and treat the excitations as classical particles with energy

$$H(y,p,t)=J[y+vt]\sin\frac{p}{\hbar}. \tag{37}$$

Here y is the coordinate of the particle, p is its momentum, and $v=I/e$ is the velocity of the constriction. For simplicity we will consider the case of dc current, $I=\text{const}$. To find the linear conductance of the quantum wire, one can limit oneself to the case of very small current, and assume $v\ll T/\hbar, J/\hbar$.

The time-dependent energy (37) should be treated as a Hamilton function, and the trajectory of the particle can, in principle, be found by solving the classical Hamilton equations. One can easily check that the quantity

$$E(y,p,t) = H(y,p,t) + pv \tag{38}$$

is an integral of motion. It has the meaning of energy of the particle in the frame moving at the speed of the constriction.

A particle with energy $\epsilon \sim T$ moving in the right direction has a very low momentum p when it is in the leads, $p/\hbar = \epsilon/J_\infty \sim T/E_F \ll 1$. Thus its integral of motion $E(y,p,t)=\epsilon$. As the particle approaches the constriction, its momentum increases, so that E retains its value despite the decrease of the bandwidth J. At small v the maximum allowed value of E in the wire is reached at $p=\pi\hbar/2$ and equals $E_{\max}=J+\frac{\pi}{2}\hbar v$. Thus at $\epsilon < J+\frac{\pi}{2}\hbar v$ the right-moving particle moves from the left lead to the right one, and its energy ϵ remains unchanged. If the energy ϵ exceeds $J+\frac{\pi}{2}\hbar v$, the particle cannot enter the wire. When its momentum reaches $\pi\hbar/2$ at a point to the left of the constriction, the particle is reflected. Deep in the left lead its momentum is very close to $\pi\hbar$. Due to the pv term in the integral of motion (38), its energy H decreases to $\epsilon - \pi\hbar v$.

Similarly, since a left-moving particle in the right lead with energy ϵ has momentum very close to $\pi\hbar$, its integral of motion (38) is $E=\epsilon+\pi\hbar v$. The condition $E<E_{\max}$ for transmission through the constriction for such particles means $\epsilon < J-\frac{\pi}{2}\hbar v$. As the particle reaches the left lead, the momentum is again near $\pi\hbar$, i.e., conservation of E results in conservation of energy $H=\epsilon$. On the other hand, particles with energies $\epsilon > J-\frac{\pi}{2}\hbar v$ are reflected back to the right lead, and their momentum on the right-moving branch is near $p=0$. Thus the energy of these particles increases from ϵ to $\epsilon + \pi\hbar v$.

To summarize, the particles in the leads with energies $\epsilon < J-\frac{\pi}{2}\hbar v$ cross the constriction region without change of energy. The particles with energies $\epsilon > J+\frac{\pi}{2}\hbar v$ are always reflected by the constriction. The ones in the left lead decrease their energy by $\pi\hbar v$, while the ones in the right lead increase their energy by the same amount, so that these contributions to the total energy of the system compensate each other. Finally, in the narrow range of energies $J-\frac{\pi}{2}\hbar v < \epsilon < J+\frac{\pi}{2}\hbar v$ the right-movers go through the constriction without change of energy, whereas the left-movers are reflected back to the right lead with energy gain $\pi\hbar v$.

The total current of left moving particles and holes in the narrow energy interval of width $\pi\hbar v$ near $\epsilon=J$ is given by $\delta\dot{N}=(2/h)(\pi\hbar v)f(J)$, where $f(\epsilon)=1/(e^{\epsilon/T}+1)$ is the Fermi function. Thus the total energy transferred to the spin excitations in unit time is

$$W^{XY} = \pi\hbar v^2 f(J) = I^2 \frac{\pi\hbar}{e^2} f(J). \tag{39}$$

Comparing this result with the Joule heat law $W=I^2R$, we obtain the spin contribution to the resistance

$$R_\sigma^{XY} = \frac{h}{2e^2} f(J). \tag{40}$$

At low temperature $T \ll J$ most of the particles have energies below J and pass through the constriction elastically. Only an exponentially small fraction of particles are reflected and contribute to the dissipation. Thus the result (40) is exponentially small at low temperatures, $R_\sigma^{XY} \simeq (h/2e^2)e^{-J/T}$. As the temperature is increased, a greater fraction of the particles are reflected by the constriction, and the R_σ^{XY} increases. In the limit $T/J \to \infty$ all the particles are reflected, and the resistance saturates at $R_\sigma^{XY}=h/4e^2$.

In this section we studied the simplified XY model, in which the z-component of coupling in the Hamiltonian (30) was neglected. Thus the result (40) cannot be applied directly to the problem of conductance of a quantum wire in the Wigner crystal regime. However, much of the physics leading to Eq. (40) can be carried over to the case of the isotropic model (30).

B. Isotropic coupling

The problem of the isotropic inhomogeneous Heisenberg spin chain (30) is far more complicated than that of the XY model (35). However, it can still be somewhat simplified by assuming that $J[y]$ is a very slowly varying function. Then each moderately long section of the spin chain can be approximated by the homogeneous Heisenberg model. The latter allows for exact solution[56] by means of Bethe ansatz. The low-energy excitations of the isotropic Heisenberg spin chain are spinons with energy spectrum[38,39]

$$\epsilon(k) = \frac{\pi J}{2} \sin k. \tag{41}$$

Although the spinons do not obey Fermi statistics, the similarity between Eq. (41) and the spectrum (36) of the excitations of the XY model enables us to find the temperature dependence of R_σ at $T \ll J$.

Indeed, most of the discussion leading to Eq. (40) did not rely on Fermi statistics of the excitations. One can apply the arguments of Sec. V A to the problem of scattering of spinons by the constriction of the band in the wire. In particular, one concludes that spinons with energies below $\pi J/2$ pass through the constriction without scattering and do not change their energy. Thus the dissipation is exponentially small at $T \ll J$, and one finds $R_\sigma \propto \exp(-\pi J/2T)$.

Since the occupation of states with high energy $\epsilon=\pi J/2$ at low temperature is exponentially small and independent of statistics, one can naively expect the resistance R_σ to be given by the low-temperature asymptotics of Eq. (40) upon replacement $J \to \pi J/2$. Then one obtains

$$R_\sigma = R_0 \exp\left(-\frac{\pi J}{2T}\right). \tag{42}$$

This approach gives the prefactor $R_0=h/2e^2$.

Unfortunately the analogy between spinons and fermion excitations of the XY model does not enable one to find the prefactor in Eq. (42). Unlike the excitations of the XY model,

the spinons interact with each other, and the energy of a spinon is affected by the presence of other spinons. In the limit $T\to 0$ the density of other spinons is small, and the energy is given by Eq. (41). At finite T the result (41) may acquire a small correction. The exponent of Eq. (42) is determined by the maximum energy of a spinon $\pi J/2$. Even a small correction to this energy may affect the prefactor R_0.

At high temperature $T\gg J$ the resistance contribution R_σ evaluated within the *XY* model approximation saturates, because in this regime all the excitations are reflected by the constriction. This feature is preserved in the model with isotropic coupling, as at $J\to 0$ the spin excitations cannot propagate through the wire. Similarly to the case of low temperature, the excitations of the spin chain are spinons. The scattering of spinons by the constriction is complicated by the fact that in the central region, where $J[l]\lesssim T$, the gas of spinons is not dilute. However, it is natural to assume that the moving constriction with $J\ll T$ backscatters all the spinons approaching it, resulting in a finite dissipation $W_\sigma = I^2 R_\sigma$.

To find the saturation value of R_σ at high temperatures we notice that in the part of the system away from the constriction, where $J[l]\simeq J_\infty \gg T$, one can still bosonize the Hamiltonian (33) and use the form (4). Inside the constriction the bosonization is not applicable, and this region should be modeled by imposing a boundary condition on the bosonic field ϕ_σ at the constriction, corresponding to the fact that there is no spin propagation between the regions of large positive and negative l. The form of the boundary condition cannot be obtained within the bosonization approach because the latter fails at $J\lesssim T$. To evaluate R_σ we assume that the exact nature of the scatterer does not affect the dissipation W_σ, as long as all the excitations are backscattered. This enables us to replace the constriction (34) of the bandwidth $D_\sigma \sim J[l]$ in the Hamiltonian (33) with a high potential barrier for the fermions. The barrier is modeled by a large backscattering term $v(a_L^\dagger a_R + a_R^\dagger a_L)$ at site $l=-q(t)$. Upon the bosonization transformation (15) this term becomes $-\tilde{v}\cos[\sqrt{2}\phi_\sigma(y) - 2k_F y]|_{y=-q(t)}$, with k_F on the lattice being $\pi/2$. Since this scattering term is very strong, $\tilde{v}\to\infty$, it pins the field $\phi_\sigma[-q(t),t]$ to the value $-\sqrt{2}k_F q(t) = -(\pi/\sqrt{2})q(t)$. This time-dependent boundary condition leads to the emission of spin waves, in analogy with Sec. III A, where the boundary condition (24) gave rise to plasmon waves (26). In the limit of weak current, $I\sim e\omega q\to 0$, the wavelength of the spin waves $\sim J_\infty/\hbar\omega$ is much larger than $q(t)$, and instead of imposing the boundary condition at $y=-q(t)$ one can impose it at $y=0$. Then the boundary condition becomes

$$\phi_\sigma(0,t) = -\frac{\pi}{\sqrt{2}} q(t). \tag{43}$$

Note that up to the inessential negative sign Eq. (43) is identical to the boundary condition (24). The respective Hamiltonians (3) and (4) are also essentially identical at low energies, as the sine-Gordon term is irrelevant. One can therefore carry over the results of Sec. III A for the dissipation of energy into plasmon waves and the resulting contribution to the resistance. Adapting Eq. (28) to the parameters of Hamiltonian (4), we find

$$R_\sigma = \frac{h}{2K_\sigma e^2}. \tag{44}$$

In the dc limit the frequency of the driving force $\omega\to 0$, and the wavelength of the spin waves is very long. Thus the parameter K_σ in Eq. (44) is taken at large distances from the constriction, where the SU(2) symmetry demands $K_\sigma = 1$. Consequently the spin contribution to the resistance in the model with isotropic coupling is given by

$$R_\sigma = \frac{h}{2e^2}. \tag{45}$$

On the other hand, the *XY* model (35) does not possess the SU(2) symmetry, and the bosonization procedure (15) gives the quadratic part of Hamiltonian (4) with $K_\sigma = 2$. Then Eq. (44) predicts $R_\sigma^{XY} = h/4e^2$, in agreement with $T\gg J$ asymptotics of Eq. (40).

VI. DISCUSSION OF THE RESULTS

The quantity most commonly measured in experiments with quantum wire devices is the linear conductance. In our theory its value is given by

$$G = \frac{1}{R_\rho + R_\sigma}, \tag{46}$$

cf. Eq. (32). The contributions R_ρ and R_σ to the resistance of the wire are determined by the properties of the charge and spin excitations of the system, respectively.

Throughout this paper we consider the case of relatively low temperature, $T\ll D_\rho \sim \hbar n u_\rho$. In this regime the contribution of the charge modes is well known: $R_\rho = h/2e^2$ (see also Sec. III B). Raising the temperature above D_ρ leads to thermal smearing of conductance plateaus. No interesting electron correlation effects are expected in this case.

At not too low electron density $n\gtrsim a_B^{-1}$ the bandwidth $D_\rho \sim D_\sigma \sim E_F$ is the only relevant energy scale of the problem. Then at $T\ll E_F$ the contribution R_σ vanishes, and the conductance takes the well-known quantized value $G = 2e^2/h$. On the other hand, in the interesting case of low density $n\ll a_B^{-1}$ another energy scale, the exchange constant J, appears in the problem. This scale is exponentially small, Eq. (11); in particular, $J\ll D_\rho$. In the limit of low temperature $T\to 0$ the contribution R_σ still vanishes. More specifically, at $T\ll J$ we predict activated temperature dependence (42) of R_σ, with activation temperature $\pi J/2$. At higher temperatures R_σ grows, and at $T\gg J$ it saturates at the universal value $R_\sigma = h/2e^2$, see Eq. (45). Combining these results with Eq. (46), we obtain

$$G = \frac{e^2}{h}, \quad J\ll T\ll D_\rho. \tag{47}$$

This is our main result. It corresponds to an additional quantized plateau of conductance of a quantum wire at low electron density. The value of the conductance at this plateau is exactly one-half of the quantized conductance $2e^2/h$.

The plateaus of conductance at e^2/h have been observed at low electron densities in several experiments.[10–13] The au-

thors of Refs. 10–13 attributed this feature to the spontaneous spin polarization in quantum wires. This interpretation contradicts the theorem by Lieb and Mattis,[57] stating that the ground state of a 1D electron system cannot be spin-polarized in the absence of magnetic field. One can hypothesize that the ferromagnetism in quantum wires is possible because the electrons are not truly one-dimensional; however, to the best of our knowledge, no such theory is available at this time. In our theory the spin structure of the Wigner crystal state is described by the Heisenberg model (10) with positive exchange constant J, corresponding to antiferromagnetic coupling. Thus the ground state of the Wigner crystal is not spin-polarized, in agreement with the theorem.[57]

The temperature dependence of the conductance of a quantum wire device obtained in this paper is similar to the behavior observed in experiments on 0.7 structure in quantum point contacts.[5–9] In agreement with experiments,[7–9] conductance (46) remains $2e^2/h$ at $T\to 0$, but develops a negative correction at finite temperature. The activated temperature dependence of the correction following from Eq. (42) is consistent with the measurements of Ref. 9. At high temperature the correction saturates, and the conductance develops a new plateau. Contrary to the experiments,[5–7] this plateau is at one-half of the quantized value $2e^2/h$, rather than at $0.7\times(2e^2/h)$. The relation between the plateau at e^2/h and the 0.7 structure was studied experimentally in Ref. 12. It was found that the quasiplateau at $0.7\times(2e^2/h)$ is observed in short wires, whereas in longer wires it shifts toward e^2/h. In this paper we assume that the wire is long, so that the parameters of the system, such as the confining potential, Fermi energy, and exchange constant J, do not change significantly at the interparticle distance. It would be interesting to generalize our approach to the case of shorter wires and see whether the physics discussed in this paper may be responsible for the 0.7 structure in quantum point contacts.

To test the relevance of our theory to the experiments[10–13] showing plateaus at e^2/h, one can check whether the experimental temperature exceeds the exchange energy J. Due to the strong exponential dependence (11) of J on the density, the uncertainty of n may make the estimation of J difficult. Instead one may be able to determine J experimentally by applying magnetic field B in the plane of the two-dimensional electron gas in the leads. Such a field does not affect the orbital motion of electrons, and couples only to their spins. If the magnetic field exceeds a certain critical value $B_c\propto J$, the spin chain becomes completely spin polarized. The magnitude of the critical field B_c can be found by considering the spin-polarized state in a strong field B with a single spin-flip excitation. The energy of such an excitation $|g|\mu_B B$ is reduced by $2J$ due to coupling to neighboring spins. (Here g is the Lande factor, and μ_B is Bohr magneton.) Thus the complete polarization occurs at $B>B_c$, where

$$B_c=\frac{2J}{|g|\mu_B}. \tag{48}$$

By measuring the critical field B_c required to achieve complete polarization of the spin chain one can determine the exchange constant J.

In the case of noninteracting electrons at zero temperature the conductance does not depend on the magnetic field and remains $2e^2/h$ until the electron gas becomes completely spin polarized at $B>B_c^{(0)}=E_F/4|g|\mu_B$. In a polarizing field only one spin channel is allowed in the wire, and the conductance reduces to e^2/h. In the case of a quantum wire at low electron density this behavior is preserved, but the step in conductance occurs at a much lower critical field (48). Indeed, although in the presence of magnetic field spinons are no longer the elementary excitations of a spin chain, at $B<B_c$ one can introduce modified elementary excitations with similar properties.[58] Then by repeating the arguments of Sec. V B one concludes that the low energy excitations present in the system at $T\to 0$ cross the wire elastically, resulting in $R_\sigma=0$ and total conductance $G=2e^2/h$. At $B>B_c$ the wire is completely spin polarized, and the spin excitations in the leads are reflected by the wire. This situation is completely analogous to the case of high temperature considered in Sec. V B. In particular, the resistance R_σ can be found by bosonizing the electron system in the leads and imposing the boundary condition (43) on the field ϕ_σ. This again leads to $R_\sigma=h/2e^2$ and reduces the conductance of the device to e^2/h. Thus one can find the critical field (48) and the exchange constant J by measuring the magnetic field at which the conductance drops from $2e^2/h$ to e^2/h.

Apart from the experiments with GaAs quantum wires, quantization of conductance at $G=e^2/h$ in the absence of magnetic field has been observed in carbon nanotubes.[59] This anomalous quantization occurs when the current is forced to flow through the narrow tip of the tube. At small radius of the nanotube the Coulomb interactions between electrons become effectively stronger, and could conceivably suppress the exchange coupling J of the electron spins below the temperature. Our result (47) would then explain the experimental data.[59]

ACKNOWLEDGMENTS

The author acknowledges helpful discussions with A. V. Andreev, A. M. Finkel'stein, L. I. Glazman, A. I. Larkin, R. de Picciotto, M. Pustilnik, and P. B. Wiegmann and the hospitality of Bell Laboratories, where part of this work was carried out. This work was supported by the U.S. DOE, Office of Science, under Contract No. W-31-109-ENG-38, by the Packard Foundation, and by NSF Grant DMR-0214149.

APPENDIX A: ESTIMATE OF THE EXCHANGE CONSTANT J

Here we estimate the exchange constant in an infinite 1D Wigner crystal with the lattice constant $b=1/n$. Following the idea of Häusler[36] we evaluate J for two spins at neighboring sites $l=0$ and $l=1$ using an approximation where the only dynamical variable is the distance $x=x_1-x_0$ between the two electrons. In this approximation, $x_0+x_1=b$ and all the other electrons ($l\neq 0,1$) are at fixed positions $x_l=lb$. Then the Coulomb potential takes the form

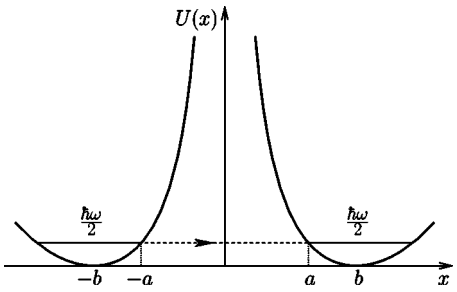

FIG. 3. The shape of the double-well potential (A2). The particle can occupy the ground state with energy $\hbar\omega/2$ in each well. Tunneling between the wells gives rise to the energy level splitting, which can be found in WKB approximation, Eq. (A4).

$$U(x)=\frac{e^2}{\varepsilon|x|}+\sum_{l\neq 0,1}\left(\frac{e^2}{\varepsilon\left|\frac{b-x}{2}-lb\right|}+\frac{e^2}{\varepsilon\left|\frac{b+x}{2}-lb\right|}\right). \tag{A1}$$

This potential has two degenerate minima at $x=\pm b$ corresponding to $x_0=0$, $x_1=b$ and $x_0=b$, $x_1=0$. In the limit of strong Coulomb potential the tunneling between these two states gives rise to exponentially small splitting ΔE of the doublet.

The ground state wave function of this system is an even function of x, and is therefore symmetric with respect to permutation $x_0\leftrightarrow x_1$, while the first excited state is antisymmetric. The two states correspond to the values of the total spin of the two-electron system $S=0$ and $S=1$, respectively. Thus the energy of the two components of the doublet can be written in terms of the electron spin operators at the two sites as $E_0+J\boldsymbol{S}_0\cdot\boldsymbol{S}_1$, where J is identified with the level splitting ΔE.

Strictly speaking the infinite series in Eq. (A1) diverges. This is due to the long range nature of the Coulomb interactions. In practice the interactions are screened at large distances by remote gates. Instead of modifying the Coulomb potential to account for the gate, it will be more convenient to simply subtract from Eq. (A1) a divergent constant $U(b)$. Then the series converges, and in the important region $|x|<3b$ the potential can be presented in analytic form as

$$U(x)=\frac{e^2}{\varepsilon b}[F(x/b)-F(1)], \tag{A2}$$

$$F(z)=\frac{1}{|z|}-2\psi\left(\frac{3-z}{2}\right)-2\psi\left(\frac{3+z}{2}\right), \tag{A3}$$

where $\psi(z)$ is the digamma function. The shape of the potential (A2) is shown in Fig. 3.

Evaluation of the energy level splitting ΔE for a particle of mass m in a double-well potential $U(x)$ is a well-known problem of quantum mechanics,[60] and the result[61] is given by

$$\Delta E=\frac{\hbar\omega}{\sqrt{e\pi}}\exp\left(-\frac{1}{\hbar}\int_{-a}^{a}\sqrt{2m[U(x)-\hbar\omega/2]}dx\right). \tag{A4}$$

Here $\omega=\sqrt{U''(b)/m}$ is the frequency of small oscillations near the minima $x=\pm b$ of the potential $U(x)$, and $x=\pm a$ are the classical turning points at energy $\hbar\omega/2$, i.e., $a=b-\sqrt{\hbar/m\omega}$, see Fig. 3.

To evaluate ΔE with the correct prefactor, one has to carefully account for the small energy $\hbar\omega/2$ in the exponential. The resulting level splitting can be written as

$$\Delta E=\frac{2}{\sqrt{\pi}}\sqrt{\hbar\omega^3 mb^2}e^{\xi}e^{-S_0}, \tag{A5}$$

where

$$S_0=\frac{1}{\hbar}\int_{-b}^{b}\sqrt{2mU(x)}dx, \tag{A6}$$

$$\xi=\int_0^1\left(\sqrt{\frac{U''(b)b^2}{2U(bz)}}-\frac{1}{1-z}\right)dz. \tag{A7}$$

An alternative solution[63] of the problem using the instanton technique leads to a result that can be also presented in the form (A5)–(A7).

In order to apply this result to the evaluation of the exchange constant J, one has to keep in mind that x is the relative position of two neighboring electrons, $x=x_0-x_1$, and replace the mass in Eqs. (A5) and (A6) with the reduced mass $m/2$. One then finds $S_0=\eta\sqrt{b/a_B}$ with the numerical coefficient

$$\eta=\int_{-1}^{1}\sqrt{F(z)-F(1)}dz\approx 2.817. \tag{A8}$$

Substitution of this result into Eq. (A5) gives the leading exponential behavior of Eq. (11).

The numerical parameter ξ defined by Eq. (A7) depends only on the shape of the barrier separating the two minima of potential $U(x)$. For the potential (A2), we find

$$\xi=\int_0^1\left(\sqrt{\frac{F''(1)}{2[F(z)-F(1)]}}-\frac{1}{1-z}\right)dz\approx -0.423. \tag{A9}$$

Substituting this result in Eq. (A5) we find the exchange constant

$$J=\frac{\kappa\hbar^2}{m\sqrt[4]{b^5a_B^3}}\exp\left(-\eta\sqrt{\frac{b}{a_B}}\right), \tag{A10}$$

with $\kappa\approx 2.203$. Expressing the prefactor in terms of the Fermi energy, we obtain Eq. (12).

It is worth mentioning that because of the singularity of the potential $U(x)$ at $x=0$, the validity of the WKB approximation used in the derivation[60] of formula (A4) is limited to $|x|\gg a_B$. Moreover, since the potential (A2) is not integrable up to the singularity, it represents an impenetrable barrier.[64] Thus the true value of the level splitting for potential (A2) is $\Delta E=0$. On the other hand, the electrons in a quantum wire

are not strictly one-dimensional due to the finite width w of the wire. As a result the singularity of the Coulomb interaction potential is cutoff at short distances $x \sim w$. In GaAs devices $w \gtrsim a_B$, which justifies the WKB approximation. In carbon nanotubes it may be possible to achieve the regime $w \ll a_B$; a more sophisticated approach to the calculation of the exchange constant J is required in this case.[65]

APPENDIX B: RESISTANCE OF A QUANTUM WIRE

Let us derive the resistance (28) of an infinite quantum wire in the regime of applied current. The wire is modeled by the Hamiltonian (3) with the time-dependent boundary condition (24). It is convenient to apply to the Hamiltonian a unitary transformation

$$U = \exp\left(- i\frac{\pi q(t)}{\sqrt{2}} \int_{-\infty}^{\infty} \Pi_\rho(x) dx \right), \tag{B1}$$

which shifts the charge field $\phi_\rho(x) \to \phi_\rho(x) + (\pi/\sqrt{2})q(t)$. As a result the boundary condition (24) is replaced with $\phi_\rho(0,t) = 0$, but the Hamiltonian (3) acquires a time-dependent perturbation

$$V = - i\hbar U^\dagger \partial_t U = - \frac{\pi\hbar}{\sqrt{2}} \dot{q}(t) \int_{-\infty}^{\infty} \Pi_\rho(x) dx. \tag{B2}$$

The perturbation (B2) leads to excitation of plasmons and to dissipation of energy into the Luttinger liquid. To find the energy W dissipated in unit time, it is convenient to diagonalize H_ρ by introducing the plasmon destruction operators

$$b_k = \int \theta(kx) \sin kx \left(\frac{1}{\pi} \sqrt{\frac{|k|}{K_\rho}} \phi_\rho(x) + i \sqrt{\frac{K_\rho}{|k|}} \Pi_\rho(x) \right) dx, \tag{B3}$$

where $\theta(y)$ is the unit step function. Note that in order to satisfy the boundary condition $\phi_\rho(0,t) = 0$ the wave functions of the plasmons were chosen in the form $\varphi_k(x) = \sqrt{2/\pi}\theta(kx)\sin kx$; positive and negative k correspond to excitations to the right and left of the boundary $x = 0$, respectively.

Upon the transformation to the new variables (B3), the two terms in the Hamiltonian take the form

$$H_\rho = \int_{-\infty}^{\infty} \hbar\omega_k b_k^\dagger b_k dk,$$

$$V = \frac{i\hbar I_0 \cos \omega t}{e\sqrt{2K_\rho}} \int_{-\infty}^{\infty} \frac{b_k - b_k^\dagger}{\sqrt{|k|}} dk. \tag{B4}$$

The perturbation V leads to both emission and absorption of plasmons with energy $\hbar\omega$. The total energy dissipated in unit time can be evaluated using the Fermi golden rule as

$$W = \frac{2\pi}{\hbar} \left(\frac{\hbar I_0}{2e\sqrt{2K_\rho}} \right)^2 \frac{2}{\hbar\omega} [(1 + f_k)\hbar\omega - f_k \hbar\omega]. \tag{B5}$$

Regardless of the values of the plasmon occupation numbers f_k, expression (B5) reduces to $W = \frac{1}{2} I_0^2 R_\rho$ with the resistance (28).

APPENDIX C: DISSIPATION OF ENERGY BY A SCATTERER IN A FERMI GAS

Let us consider the dissipation of energy in a noninteracting Fermi gas in the presence of a moving scatterer. We assume that the single-particle Hamiltonian has the general form

$$H(y,p,t) = H_0(y + q_0 \sin \omega t, p). \tag{C1}$$

Here the Hermitian operator $H_0(y,p)$ is independent of the coordinate y in the regions corresponding to the leads, $y \to \pm\infty$. The Hamiltonian (35) obviously satisfies these conditions for smoothly varying $J[y]$ after the discrete site number l is replaced by a continuous coordinate y. The y-dependent central part of the Hamiltonian $H_0(y,p)$ can be viewed as a scatterer with energy-dependent reflection coefficient $\mathcal{R}(\epsilon)$. Condition (C1) implies that the position of the scatterer oscillates with amplitude q_0.

In the limit of small q_0 one can expand Eq. (C1) and present the Hamiltonian as

$$H(y,p,t) = H_0(y,p) + q_0 \sin \omega t \partial_y H_0(y,p). \tag{C2}$$

The time-dependent perturbation leads to absorption and emission of energy quanta $\hbar\omega$ by the fermions. The rates of these processes may be found using the Fermi golden rule, and one obtains the increase W of the energy of the system in unit time in the form

$$W = \frac{2\pi}{\hbar} \hbar\omega \int\int dk dk' \left| \frac{q_0}{2} [\partial_y H_0]_{kk'} \right|^2 \times [f(\epsilon_k) - f(\epsilon_k')] \delta(\epsilon_k - \epsilon_{k'} + \hbar\omega). \tag{C3}$$

Here k labels the eigenstates of Hamiltonian H_0 with energies ϵ_k. The occupation numbers of these states are given by the Fermi function $f(\epsilon_k)$. The eigenfunctions have scattering wave asymptotics

$$\psi_k(y) = \frac{1}{\sqrt{2\pi}} \times \begin{cases} e^{iky} + r_k e^{-iky} & \text{at } y \to -\infty, \\ t_k e^{iky} & \text{at } y \to +\infty \end{cases} \tag{C4}$$

for positive k and

$$\psi_k(y) = \frac{1}{\sqrt{2\pi}} \times \begin{cases} t_k e^{iky} & \text{at } y \to -\infty, \\ e^{iky} + r_k e^{-iky} & \text{at } y \to +\infty \end{cases} \tag{C5}$$

for negative k. Here r_k and t_k are the reflection and transmission amplitudes; the reflection coefficient is defined as $\mathcal{R}(\epsilon_k) = |r_k|^2$.

In the limit of low frequency $\omega \to 0$ expression (C3) can be further simplified,

$$W = \frac{\pi(\omega q_0)^2}{\hbar v_F^2} \int d\epsilon_k [-f'(\epsilon_k)][\zeta_+(\epsilon_k) + \zeta_-(\epsilon_k)]. \tag{C6}$$

Here we have approximated the energies near the Fermi level as $\epsilon_k = \hbar v_F(|k| - k_F)$, accounted for the double degeneracy of the energy levels ϵ_k, and introduced

$$\zeta_\pm(\epsilon_k) = \lim_{k' \to \pm k} |[\partial_y H_0]_{kk'}|^2. \tag{C7}$$

The matrix element $[\partial_y H_0]_{k,k'}$ is defined as

$$[\partial_y H_0]_{kk'} = \int dy \psi^*_{k'}(y)[\partial_y H_0]\psi_k(y). \quad \text{(C8)}$$

Integrating by parts and taking advantage of the fact that ψ_k is an eigenfunction of H_0, we find

$$[\partial_y H_0]_{kk'} = (\epsilon_k - \epsilon_{k'}) \int dy \psi^*_{k'}(y)\partial_y \psi_k(y). \quad \text{(C9)}$$

To evaluate $\zeta_\pm(\epsilon_k)$ we need to find the divergent at $k' \to \pm k$ part of the integral in Eq. (C9). Since the divergences originate at $y \to \pm\infty$, one can use the scattering wave asymptotics (C4) and (C5) in Eq. (C9). This results in

$$\zeta_+(\epsilon_k) = \frac{1}{\pi^2}(\hbar v_F k_F)^2[\mathcal{R}(\epsilon_k)]^2, \quad \text{(C10)}$$

$$\zeta_-(\epsilon_k) = \frac{1}{\pi^2}(\hbar v_F k_F)^2 \mathcal{R}(\epsilon_k)[1 - \mathcal{R}(\epsilon_k)]. \quad \text{(C11)}$$

Substituting these results into Eq. (C6), we find

$$W = \frac{\hbar}{\pi}(\omega q_0)^2 k_F^2 \int d\epsilon[-f'(\epsilon)]\mathcal{R}(\epsilon). \quad \text{(C12)}$$

To apply this result to the evaluation of the spin contribution to the resistance within the *XY* model approximation, one should substitute $\omega q_0 = I_0/e$ and $k_F = \pi/2$. Then Eq. (C12) takes the form

$$W = \frac{1}{2} I_0^2 R_\sigma^{XY}, \quad R_\sigma^{XY} = \frac{h}{4e^2} \int d\epsilon[-f'(\epsilon)]\mathcal{R}(\epsilon). \quad \text{(C13)}$$

The result for the resistance coincides with Eq. (40) for the appropriate reflection coefficient $\mathcal{R}(\epsilon) = \theta(|\epsilon| - J)$.

[1] B. J. van Wees, H. van Houten, C. W. J. Beenakker, J. G. Williamson, L. P. Kouwenhoven, D. van der Marel, and C. T. Foxon, Phys. Rev. Lett. **60**, 848 (1988).

[2] D. A. Wharam, T. J. Thornton, R. Newbury, M. Pepper, H. Ahmed, J. E. F. Frost, D. G. Hasko, D. C. Peacock, D. A. Ritchie, and G. A. C. Jones, J. Phys. C **21**, L209 (1988).

[3] S. Tarucha, T. Honda, and T. Saku, Solid State Commun. **94**, 413 (1995).

[4] A. Yacoby, H. L. Stormer, N. S. Wingreen, L. N. Pfeiffer, K. W. Baldwin, and K. W. West, Phys. Rev. Lett. **77**, 4612 (1996).

[5] K. J. Thomas, J. T. Nicholls, M. Y. Simmons, M. Pepper, D. R. Mace, and D. A. Ritchie, Phys. Rev. Lett. **77**, 135 (1996).

[6] K. J. Thomas, J. T. Nicholls, N. J. Appleyard, M. Y. Simmons, M. Pepper, D. R. Mace, W. R. Tribe, and D. A. Ritchie, Phys. Rev. B **58**, 4846 (1998).

[7] S. M. Cronenwett, H. J. Lynch, D. Goldhaber-Gordon, L. P. Kouwenhoven, C. M. Marcus, K. Hirose, N. S. Wingreen, and V. Umansky, Phys. Rev. Lett. **88**, 226805 (2002).

[8] A. Kristensen, J. Bo Jensen, M. Zaffalon, C. B. Sørensen, P. E. Lindelof, M. Michel, and A. Forchel, J. Appl. Phys. **83**, 607 (1998).

[9] A. Kristensen, H. Bruus, A. E. Hansen, J. B. Jensen, P. E. Lindelof, C. J. Marckmann, J. Nygard, C. B. Sørensen, F. Beuscher, A. Forchel, and M. Michel, Phys. Rev. B **62**, 10950 (2000).

[10] B. E. Kane, G. R. Facer, A. S. Dzurak, N. E. Lumpkin, R. G. Clark, L. N. Pfeiffer, and K. W. West, Appl. Phys. Lett. **72**, 3506 (1998).

[11] K. J. Thomas, J. T. Nicholls, M. Pepper, W. R. Tribe, M. Y. Simmons, and D. A. Ritchie, Phys. Rev. B **61**, R13365 (2000).

[12] D. J. Reilly, G. R. Facer, A. S. Dzurak, B. E. Kane, R. G. Clark, P. J. Stiles, R. G. Clark, A. R. Hamilton, J. L. O'Brien, N. E. Lumpkin, L. N. Pfeiffer, and K. W. West, Phys. Rev. B **63**, 121311(R) (2001).

[13] D. J. Reilly, T. M. Buehler, J. L. O'Brien, A. R. Hamilton, A. S. Dzurak, R. G. Clark, B. E. Kane, L. N. Pfeiffer, and K. W. West, Phys. Rev. Lett. **89**, 246801 (2002).

[14] C.-K. Wang and K.-F. Berggren, Phys. Rev. B **57**, 4552 (1998).

[15] H. Bruus and K. Flensberg, Semicond. Sci. Technol. **13**, A30 (1998).

[16] S. M. Reimann, M. Koskinen, and M. Manninen, Phys. Rev. B **59**, 1613 (1999).

[17] B. Spivak and F. Zhou, Phys. Rev. B **61**, 16730 (2000).

[18] V. V. Flambaum and M. Yu. Kuchiev, Phys. Rev. B **61**, R7869 (2000).

[19] T. Rejec, A. Ramšak, and J. H. Jefferson, Phys. Rev. B **62**, 12985 (2000).

[20] H. Bruus, V. V. Cheianov, and K. Flensberg, Physica E (Amsterdam) **10**, 97 (2001).

[21] K. Hirose, S. S. Li, and N. S. Wingreen, Phys. Rev. B **63**, 033315 (2001).

[22] O. P. Sushkov, Phys. Rev. B **64**, 155319 (2001); **67**, 195318 (2003).

[23] Y. Tokura and A. Khaetskii, Physica E (Amsterdam) **12**, 711 (2002).

[24] Y. Meir, K. Hirose, and N. S. Wingreen, Phys. Rev. Lett. **89**, 196802 (2002).

[25] G. Seelig and K. A. Matveev, Phys. Rev. Lett. **90**, 176804 (2003).

[26] A. A. Starikov, I. I. Yakimenko, and K.-F. Berggren, Phys. Rev. B **67**, 235319 (2003).

[27] E. Wigner, Phys. Rev. **46**, 1002 (1934); Trans. Faraday Soc. **34**, 678 (1938).

[28] K. A. Matveev, Phys. Rev. Lett. **92**, 106801 (2004).

[29] I. E. Dzyaloshinskii and A. I. Larkin, Sov. Phys. JETP **38**, 202 (1974).

[30] C. F. Coll III, Phys. Rev. B **9**, 2150 (1974).

[31] F. D. M. Haldane, J. Phys. C **14**, 2585 (1981).

[32] H. J. Schulz, G. Cuniberti, and P. Pieri, in *Field Theories for Low-Dimensional Condensed Matter Systems*, edited by G. Morandi *et al.* (Springer-Verlag, New York, 2000).

[33] T. Giamarchi, *Quantum Physics in One Dimension* (Clarendon Press, Oxford, 2004).

[34] L. I. Glazman, I. M. Ruzin, and B. I. Shklovskii, Phys. Rev. B **45**, 8454 (1992).

[35] See, e.g., J. H. Jefferson and W. Häusler, Phys. Rev. B **54**, 4936 (1996).

[36] W. Häusler, Z. Phys. B: Condens. Matter **99**, 551 (1996).
[37] The numerical coefficients in the Hamiltonian (4) are different from those obtained by conventional bosonization (Refs. 32 and 33) of the Heisenberg model. The discrepancy is due to the fact that the standard procedure uses different bosonic fields $\phi = \phi_\sigma/\sqrt{2}$ and $\theta = \sqrt{2}\theta_\sigma$.
[38] J. des Cloizeaux and J. J. Pearson, Phys. Rev. **128**, 2131 (1962).
[39] L. D. Faddeev and L. A. Takhtajan, Phys. Lett. **85A**, 375 (1981).
[40] One can easily check that the derivation of Eq. (9) is valid not only for a Wigner crystal, but for any translation-invariant model of interacting electrons.
[41] V. V. Cheianov and M. B. Zvonarev, J. Phys. A **37**, 2261 (2004); Phys. Rev. Lett. **92**, 176401 (2004).
[42] G. A. Fiete and L. Balents, Phys. Rev. Lett. **93**, 226401 (2004).
[43] M. Ogata and H. Shiba, Phys. Rev. B **41**, 2326 (1990).
[44] H. Shiba and M. Ogata, in *Strongly Correlated Electron Systems II*, edited by G. Baskaran, A. E. Ruckenstein, E. Tosatti, and Y. Lu (World Scientific, Singapore, 1991), p. 31.
[45] K. A. Matveev (unpublished).
[46] C. L. Kane and M. P. A. Fisher, Phys. Rev. B **46**, 15233 (1992).
[47] A. Furusaki and N. Nagaosa, Phys. Rev. B **47**, 4631 (1993).
[48] The asymptotics at $x \to \pm\infty$ in Eq. (26) are chosen to correspond to outgoing plasmon wave.
[49] Experiments with cleaved edge overgrowth wires (Ref. 4) show quantization below $2e^2/h$, but this value is still independent of the electron density. The reduction of the quantized value was attributed to the imperfect coupling of the wire to the leads (Ref. 50).
[50] R. de Picciotto, H. L. Stormer, A. Yacoby, L. N. Pfeiffer, K. W. Baldwin, and K. W. West, Phys. Rev. Lett. **85**, 1730 (2000).
[51] D. L. Maslov and M. Stone, Phys. Rev. B **52**, R5539 (1995).
[52] V. V. Ponomarenko, Phys. Rev. B **52**, R8666 (1995).
[53] I. Safi and H. J. Schulz, Phys. Rev. B **52**, R17040 (1995).
[54] It is worth mentioning that the violation of the spin-charge separation in Eq. (30) is due to the inhomogeneity of the system. In the homogeneous case $J = \text{const}$, and the spin-charge separation is restored.
[55] L. B. Ioffe and A. I. Larkin, Phys. Rev. B **39**, 8988 (1989).
[56] H. A. Bethe, Z. Phys. **71**, 205 (1931).
[57] E. Lieb and D. Mattis, Phys. Rev. **125**, 164 (1962).
[58] M. Karbach and G. Müller, Phys. Rev. B **62**, 14871 (2000).
[59] S. Frank, P. Poncharal, Z. L. Wang, and W. A. de Heer, Science **280**, 1744 (1998).
[60] L. D. Landau and E. M. Lifshitz, *Quantum Mechanics* (Butterworth-Heinemann, Oxford, 1997), p. 183.
[61] The standard solution (Ref. 60) applies the WKB approximation to the ground states of the oscillatory potentials near the minima of $U(x)$. As a result it underestimates the level splitting (A4) by a factor (Ref. 62) of $\sqrt{\pi/e} \approx 1.075$.
[62] W. H. Furry, Phys. Rev. **71**, 360 (1947).
[63] S. Coleman, *Aspects of Symmetry* (Cambridge University Press, Cambridge, 1985), p. 341.
[64] M. Andrews, Am. J. Phys. **44**, 1064 (1976).
[65] M. M. Fogler, cond-mat/0408079.